

Absorption of Ethylene on Membranes Containing Potassium Permanganate Loaded into Alumina-Nanoparticle-Incorporated Alumina/Carbon Nanofibers

Ashkan Tirgar, Daewoo Han,[✉] and Andrew J. Steckl^{*✉}

Nanoelectronics Laboratory, Department of Electrical Engineering and Computer Science, University of Cincinnati, Cincinnati, Ohio 45221-0030, United States

S Supporting Information

ABSTRACT: Ethylene is a natural aging hormone in plants, and controlling its concentration has long been a subject of research aimed at reducing wastage during packaging, transport, and storage. We report on packaging membranes, produced by electrospinning, that act as efficient carriers for potassium permanganate (PPM), a widely used ethylene oxidant. PPM salt loaded on membranes composed of alumina nanofibers incorporating alumina nanoparticles outperform other absorber systems and oxidize up to 73% of ethylene within 25 min. Membrane absorption of ethylene generated by avocados was totally quenched in 21 h, and a nearly zero ethylene concentration was observed for more than 5 days. By comparison, the control experiments exhibited a concentration of 53% of the initial value after 21 h and 31% on day 5. A high surface area of the alumina nanofiber membranes provides high capacity for ethylene absorption over a long period of time. In combination with other properties, such as planar form, flexibility, ease of handling, and lightweight, these membranes are a highly desirable component of packaging materials engineered to enhance product lifetime.

KEYWORDS: *electrospinning, potassium permanganate, alumina nanoparticle, alumina fiber, ethylene absorption, ripening prevention*

1. INTRODUCTION

Climacteric fruits, such as banana, tomato, avocado, kiwi, apples, apricots, and blackberries, produce ethylene (C₂H₄), which regulates the plant growth and ripening process.^{1–19} The ripening process, normally described by flesh softening, color change, and production of aromas, leads to the loss of eating quality in fruits and reduces their storage life. Even non-climacteric fruits, such as strawberries and grapes, have shown acceleration in the ripening process upon exposure to exogenous ethylene.²⁰

Previously, various methods and materials have been suggested to control the ethylene level. Sorbents, such as zeolite and carbon, have been successfully used to adsorb ethylene,^{19,21–23} but these materials only transfer it to another phase without any chemical destruction of ethylene. Use of catalytic materials, such as palladium and TiO₂ nanoparticles, have been reported as an alternative ethylene control method. However, they are not favored in these applications because palladium is an expensive material and TiO₂ requires ultraviolet (UV) light to react with ethylene. The most common ethylene control absorbent used in the fruit industry consists of strong oxidants, such as potassium permanganate (PPM), loaded on inert carrier materials, such as alumina^{24–27} or diatomaceous earth.^{28,19,29,30} PPM is extensively used in many applications, such as the absorber component of ethylene control systems,³¹ water treatment,³² and antimicrobial agent in antiseptic products.³³ A chemical leach study is recommended after developing any system containing PPM to select the right packaging material/structure that would not allow more than a “do not use” concentration of ~0.1 g of PPM (for a 75 kg person)³⁴ in one exposure from contaminated fruits/produce.

Our nanofiber membranes have an inherent advantage because they can be easily sandwiched between PPM-free (electrospun) membranes or any other desired packaging layers. Typically, an aqueous solution of the permanganate salt is loaded into/on the carrier substrate of interest to obtain an ethylene absorber system. In our paper, the term “absorption” is used when ethylene molecules are hydroxylated by reacting with oxidants.

To be used as a PPM carrier, the material must be inert to the chemical reaction with PPM and provide a porous structure with a high surface area. To date, PPM carriers for absorbing ethylene have been developed in different forms of beads, films, and liners. As a result of their physical form, the beads are placed inside small pouches made of gas-permeable materials.^{19,29,30,35–41} Therefore, they can only provide ethylene absorption in a very limited area around the pouch. The self-supporting membranes demonstrated in our report can address this issue by serving as a PPM carrier that can be used as a packaging material for either individual fruits or the entire batch set of fruits. In addition, because the natural convection and diffusion are the only driving forces displacing ethylene molecules, the efficiency of all different forms of absorption systems (bead, film, and liner) would depend upon their surface area where the contact and, thus, reaction between ethylene and the oxidant occurs. A study of 21 different carrier materials has demonstrated that carriers with lower bulk densities and higher salt uptake capacity are more efficient in reducing

Received: October 31, 2017

Revised: April 18, 2018

Accepted: April 19, 2018

Published: May 11, 2018

ethylene levels. Our membranes provide a uniquely large surface area and are fabricated using fiber electrospinning, a simple but versatile technique that can be a cost-effective method for making PPM carriers.

Electrospinning^{42–44} is an extremely versatile technique for the fabrication of light and flexible free-standing porous fiber membranes made of a wide range and combinations of materials. The diameter of fibers produced by electrospinning ranges from tens of nanometers to micrometers depending upon the solution parameters (viscosity, conductivity, vapor pressure, etc.) and process parameters (voltage, distance, flow rate, etc.). This technique has also been used for the fabrication of coaxial and triaxial fibers required in specific applications.^{45,46} The electrospinning setup is composed of a high-voltage power supply connecting a spinneret and a collecting substrate that is grounded. The applied electric field provides a force for stretching a liquid out of the droplet at the tip of the nozzle. The liquid jet travels the distance between the spinneret and the collector, while it undergoes whipping and bending instabilities that elongate the jet, and eventually forms a nearly dry mesh of fibers, with a high surface/volume ratio.

Here, we report the first demonstration of using an electrospun nanofiber membrane loaded with a permanganate ethylene absorber to prevent food ripening. A summary of our approaches for making ethylene absorber membranes is illustrated in Figure 1. Alumina nanoparticle (ANP)-incorporated

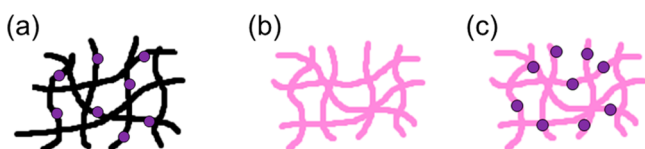


Figure 1. Basic concept diagrams: PPM loaded on (a) ANP-incorporated CNFs, (b) ANF membrane, and (c) ANP-incorporated ANF membrane.

rated carbon nanofibers (CNFs) after PPM casting are illustrated in Figure 1a. These membranes were electrospun from an ANP-dispersed polyacrylonitrile (PAN) solution followed by a two-step carbonization process that converts PAN polymer fibers to carbon fibers. The carbonization step is necessary because PPM is a very strong oxidizing agent that will be inactivated by reduction upon contact with most polymers

and solvents commonly used in electrospinning. Our second approach, illustrated in Figure 1b, uses alumina nanofibers (ANFs) fabricated by electrospinning a polymer solution containing aluminum acetate (AlAc), followed by a calcination process in air to convert AlAc to alumina. Alumina is widely used in industrial compounds as an adsorbent, abrasive, and water-proofing agent and in lubricants.⁴⁷ The oral median lethal dose (LD₅₀) value for aluminum compounds is between 162 and 980 mg/kg.⁴⁸ Hence, on the basis of the weight of our developed membranes and the concentration of alumina in them, they should not expose any risk to the health of consumers. Finally, Figure 1c illustrates ANFs impregnated with ANPs to improve their efficiency as a PPM carrier. We have investigated the relationship between the ANP concentration and the ethylene absorption capacity of ANP-incorporated ANFs. The results indicate that the ethylene absorption capacity of our membranes can outperform other well-known absorber systems, such as blueapple absorber and PPM-loaded alumina beads. Further, the membrane absorption capacity can be easily tuned by controlling the amount of ANPs incorporated into the fibers. Furthermore, our membranes possess properties, such as planar form, flexibility, ease of handling, and lightweight, that are attractive for many applications, enabling potential users to easily customize the absorption capacity and rate of absorption based on their needs.

2. EXPERIMENTAL SECTION

2.1. Materials. PAN ($M_w = 150$ kDa), polyvinylpyrrolidone (PVP, $M_w = 360$ kDa), aluminum oxide nanopowder (diameter of <50 nm), and AlAc (dibasic) were purchased from Sigma-Aldrich (St. Louis, MO, U.S.A.). *N,N*-Dimethylformamide (DMF, 99.8% purity), formic acid (FA, 88%), and ethanol (200 proof) were purchased from Fisher Scientific (Pittsburgh, PA, U.S.A.). PPM ($\geq 99.0\%$) was purchased from two different sources, Sigma-Aldrich and Alfa Aesar (Haverhill, MA, U.S.A.). Activated alumina beads ($1/8$ in. diameter) were purchased from Delta Adsorbents (Chicago, IL, U.S.A.). A commercial ethylene absorber named blueapple Freshness Ball (refill kit) was used for comparison, which was purchased from Kitchen Kapors (Cherry Hill, NJ, U.S.A.). All materials were used as received without any further modification.

2.2. Sample Preparation. Production of electrospun fibers was performed using a conventional vertical electrospinning setup composed of a high-voltage power supply, syringe set placed on a syringe pump, and conducting substrate. A high-voltage supply was clipped between the collector and a 22 g blunt needle, which was used as a spinneret Luer locked to a 5 mL plastic syringe containing the

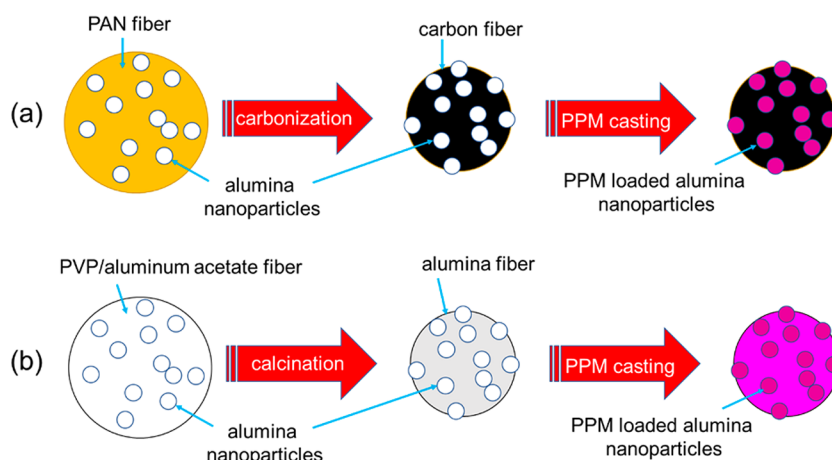


Figure 2. Production of ANP-incorporated fibers followed by PPM loading (cross-sectional view): (a) carbon fibers and (b) alumina fibers.

electrospinning solution. The distance between the spinneret tip and a grounded aluminum foil used for collection of nanofibers (collection distance) was 20 cm in all cases.

To produce CNFs, we first prepared polymer membranes by electrospinning PAN (9 wt %) in DMF solution at a flow rate and bias voltage of 1.5 mL/h and 18.5 kV, respectively. The polymer fibers then underwent a stabilization process at 260 °C (ramp rate of 2 °C/min) for 3 h, followed by carbonization at 1000 °C (ramp rate of 5 °C/min) for 1 h in the presence of argon gas with a constant flow rate of 2 standard cubic feet per hour (SCFH). As illustrated briefly in Figure 2a, ANP-incorporated CNFs were achieved by electrospinning ANP-dispersed PAN/DMF solution and performing the sequential stabilization and calcination processes on ANP-incorporated PAN fibers. Up to 15 wt % (with respect to solvent) of ANPs was very well dispersed in the PAN/DMF solution after stirring the solution for several hours. The resulting solutions were electrospun smoothly with a collection distance of 15–20 cm, flow rate of 0.5–1.2 mL/h, and bias voltage of 12–19 kV. Finally, a 2% (w/v) PPM aqueous solution was casted on the membranes using a pipet, and then the membranes were dried in a vacuum oven at room temperature (RT). It is worth mentioning that stabilization and carbonization processes reduce the fiber diameter significantly, leading to a larger ratio between ANPs and carbon material than the ratio between ANPs and PAN polymer in the original membrane.

To make ANFs, AlAc solution was prepared by dissolving 2.22 g of AlAc into the mixture of FA (2.22 g) and deionized (DI) water (5.56 g) and then was blended homogeneously with 10 g of 20% (w/w) PVP in ethanol solution. A syringe containing the solution was pumped at 0.7 mL/h, and fibers were obtained under 15 kV bias voltage within a 20 cm collection distance. Electrospun membranes were then calcined at 700 °C for 1 h in air (ramp rate of 10 °C/min), resulting in shrinkage and weight loss of membranes. In the final step, PPM aqueous solution (2%, w/v) was cast dropwise and membranes were vacuum-dried at RT. As illustrated in Figure 2b, the same procedure was followed for making ANP-incorporated ANFs, except that the starting electrospinning solution contained a uniform dispersion of ANPs. The weight of ANPs added to the 20 g of total solution was 1 or 2 g to obtain 5 or 10% (w/w) of ANP in the solution, respectively. In the rest of this paper, to simplify the terms, we refer to the fiber membranes obtained from these solutions as 5 or 10% ANP-incorporated ANFs.

For the results to be comparable, we made every effort to be consistent in the amount of absorber materials used in each experiment. In each case, we used ~140 mg of carrier material loaded with ~30 mg of PPM. All membranes were cut to have a similar apparent area of ~28.1 cm² (mostly shaped as a 5.3 cm square). In the case of ANP-incorporated membranes, the carrier weight is the total weight of nanoparticles and fiber material together. Alumina beads and nanoparticles were also weighed to be ~140 mg before being loaded with PPM. The concentration of PPM aqueous solution varied on the basis of the solution uptake capacity of each carrier, leading to 2 and 5% (w/v) PPM solutions used for membranes and alumina beads, respectively. A total of 1.5 mL of 2% PPM solution was loaded on membranes, while the PPM loading of alumina beads was performed by repeating 3 times of loading and vacuum drying processes with a higher concentration of PPM solution (5%, w/v) as a result of the limited water uptake capacity of alumina beads. The amount of blueapple absorber used in gas experiments was determined to be 190 mg, which is 20 mg more than the weight of PPM-loaded membranes or beads after complete drying. All as-spun membranes have a size of 10 × 10 cm² before any heat treatment. Each case has been performed at least 2 times to evaluate the reproducibility.

2.3. Fiber Morphologies. Scanning electron microscopy (SEM) was performed (EVEX SX-30 mini-SEM) to observe the fiber morphology and structure. To provide the required sample conductivity for SEM imaging, insulating samples were coated with a very thin (<10 nm) gold layer (Denton Vacuum Desk II sputtering system) at 50–60 mTorr pressure for 50 s.

2.4. Ethylene Absorption Kinetics on Membranes. The ethylene level was monitored using F950 three gas analyzer (Felix

Instruments, Camas, WA, U.S.A.). This analyzer uses an electrochemical sensor⁴⁹ for detection of ethylene and has a fine resolution, low detection limit, and wide detection range of 0.1, 0.2, and 0–200 ppm, respectively. The gas is pumped into the sensor of the analyzer at an average flow rate of 70 mL/min. To measure ethylene absorption capability of samples, gas-sealed bags were prepared by incorporating a rubber septum used as a gas injection port and for inserting the analyzer probe into the bags. Gas-sealed bags were filled with ~3 L of air, and 60 μL of pure ethylene gas was injected into the sealed bag using a Hamilton gastight sample-lock syringe. After waiting a few minutes to allow ethylene to spread uniformly inside the bag, the analyzer probe is inserted into the bag and the ethylene level analysis starts. It usually takes ~3 min for the ethylene level to reach a plateau in the range of 18–23 ppm. During this time, the absorber inside the bag is kept isolated from the ethylene/air by pressing it in the corner of the bag. After that, the isolated membrane is released and starts to interact with the gas inside the bag. The experiment time in this case (short-term experiments) is limited because the analyzer continuously samples the air in the sealed bags, and the bags run out of air after ~40 min. However, in the long term (6 days) experiments with fruits, the bags had an opening to allow for breathing, and the measurements were taken at random time points, with each measurement lasting 3–5 min until the desired stability in the output of the analyzer sensor is obtained. All experiments were performed in normal room conditions (20.3 °C, relative humidity of 39–40%, 19.5% oxygen, and 0.036% carbon dioxide).

2.5. Membrane Absorption of Ethylene Produced by Fruits.

The long-term (5 days) ethylene absorption capability of our membranes was measured by placing a membranes and target fruits in a bag that has an opening to allow for breathing of the fruit and prevent rotting. The effect of a 5% ANP-incorporated ANF membrane on a single avocado weighing ~153 g as the target fruit was evaluated. Bags used in the experiment have ~1.1 L volume with a 1 in. opening. Four fresh avocados were picked on the day of the experiment and placed in four separate bags: three bags with 5% ANP-incorporated ANF membranes ($n = 3$) and one bag without membranes as a control. The 5% ANP-incorporated ANF membrane was chosen as a result of its suitable absorption capacity while possessing more mechanical flexibility than its 10% ANP-incorporated ANF counterpart.

An instance of the impact of our developed membranes in extending the shelf life of fruits was examined using bananas as the target fruit. Two tests were performed in parallel, with bananas placed in separate zip-lock bags. One bag contained a 0.7 g membrane made of 5% ANP-incorporated ANFs loaded with PPM. A control test with no absorber in the bag was performed in parallel under the same conditions. Bananas for this test were selected from a single bunch to ensure minimum difference between their initial condition and treatment history.

3. RESULTS

3.1. ANP-Incorporated CNF Membrane. CNFs have been widely used in many applications, such as electrode material for batteries,^{50,51} electrochemical sensors,⁵² and supercapacitors,⁵³ because of their excellent electrochemical and mechanical properties. As described in Figures S1 and S2 of the Supporting Information, polymers are not suitable as a PPM carrier material because PPM can be deactivated by chemical reduction with polymer carriers. Therefore, PPM-based ethylene absorbers require chemically inert carrier materials. While CNFs are a good potential candidate for this purpose, our experiments indicate that PPM-loaded CNFs are not effective in ethylene absorption, as shown in Figure S3 of the Supporting Information. This can be attributed to the loss of the PPM-coated surface area as a result of the formation of large salt crystals observed on the dried carbon fibers after PPM casting. To resolve this issue, we impregnated CNFs with ANPs by electrospinning a dispersion of ANPs (9 wt %) in the PAN

(9 wt %)/DMF solution. ANPs show a stable uniform dispersion in solution, and thus, we were able to obtain PAN fibers accommodating ANPs on the surface and inside fibers, as shown in Figure 3a. The heat treatment used to convert ANP-

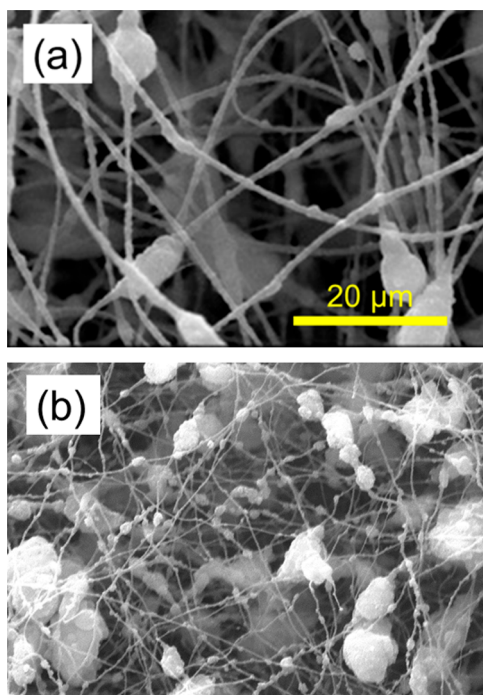


Figure 3. SEM microphotographs: (a) as-spun ANP-incorporated PAN polymer fibers at 1:1 (w/w) fibers and (b) calcined ANP-incorporated CNFs. The same magnification was used for both SEM images.

incorporated PAN to carbon materials reduced the fiber diameter, as shown in Figure 3b, and decreased the weight of the membrane to $\sim 63\%$ on average for seven fabricated membranes. The size of the membrane decreases to $\sim 42\%$, from a $10 \times 10 \text{ cm}^2$ as-spun membrane to a $6.5 \times 6.5 \text{ cm}^2$ carbon membrane. After carbonization, the ANPs become more exposed to the surface of fibers as a result of reduction in the fiber diameter. Occasional aggregations along the fibers are observed. This aggregation of nanoparticles may adversely affect the absorption capacity of membranes but can be resolved with more individually dispersed ANPs in solution achieved by high power sonication. Assuming that the weight of ANPs remains constant during the heat treatment process, the weight change of the membranes can be attributed to the weight loss of the fibers. This results in an increase in the weight ratio of ANPs to carbon fiber material from 1:1 to 3.57:1. While CNFs do not make a significant impact on the final weight of the absorber material, their strength at a relatively low weight is sufficient to produce a durable and flexible scaffold for the nanoparticles. This allows for the transformation of the ANP absorber from the powder form to the easy handling membrane form that can provide uniform absorption all around it. The results shown in Figure 4 indicate the efficiency of ANP-incorporated CNF membranes by absorbing 13.6% of the initial ethylene amount in the first 12 min. By comparison, ANPs loaded with PPM (without any carrier membrane) have a comparable ethylene absorption. For the ANP only case, the ethylene absorption started later than the ANP-incorporated CNF, leading to a higher ethylene level

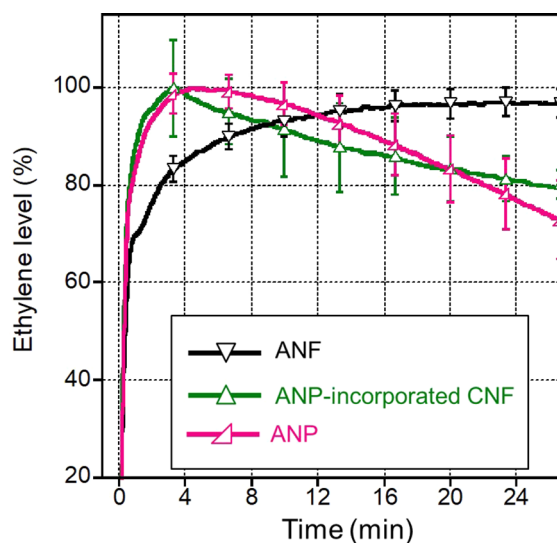


Figure 4. Ethylene absorption profiles of the ANP-incorporated CNF membrane, alumina nanopowder, and ANF membrane [vertical bars represent the standard deviation (SD) of three tests].

compared to ANP-incorporated CNF. However, in the longer time after 15 min, because ANP only has a faster ethylene absorption rate, it presented better ethylene absorption than that of the ANP-incorporated CNF.

3.2. ANF Membrane. Because it is apparent that alumina is the best carrier material to maximize the PPM performance, we fabricated ANFs by electrospinning, followed by the calcination process (see section 2.2 for more details). Images of as-spun and calcined fibers in Figure 5a demonstrate a shrinkage of the

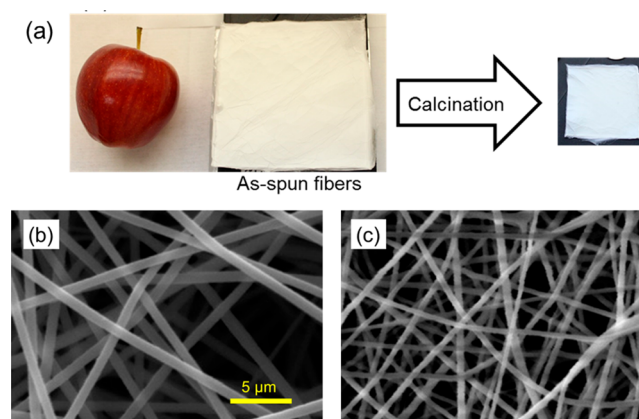


Figure 5. Size of electrospun membranes and diameter of fibers change during calcination: (a) camera images of the as-spun PVP/AlAc membrane and when converted into the alumina membrane via calcination. The length of the membrane is similar to the size of an apple. SEM microphotographs of (b) PVP/AlAc fibers and (c) calcined alumina fibers. The same magnification was used for both SEM images.

membrane. It causes a $\sim 50\%$ average reduction in the size and $\sim 80\%$ average reduction in the weight among the seven membranes investigated. SEM images of fibers shown in panels b and c of Figure 5 indicate a 795 nm diameter for as-spun fibers versus a 440 nm diameter for ANFs.

The result of ethylene absorption through PPM-loaded ANF membranes is reported in Figure 4. The average ethylene absorption capacity in this experiment is much less than

expected, showing negligible absorption during the first 20 min after release of the membrane, followed by only a 4.3% drop in the ethylene level at the end of the 40 min test period. This can be due to the lack of enough functional hydroxyl groups on the surface of alumina fibers that can bind with PPM salt ions. In fact, crystallized chunks of PPM salt incapable of binding to alumina fibers can be observed on PPM-loaded ANF membranes after drying. Although a solution to this problem may be achieved using a different calcination process and/or aluminum precursor to obtain more functional hydroxyl groups on the fiber surface, we addressed this issue by incorporating ANPs into ANFs. This was achieved using a similar procedure to that used to fabricate ANP-incorporated CNFs, namely, dispersing ANPs in the electrospinning solution. The ANP-incorporated ANFs show few salt crystals, indicating a higher binding affinity between fiber material and PPM salt. This is also confirmed from the stronger purple color of the ANP-incorporated ANF membrane compared to the ANF membrane when they have the same weight, size, and loaded PPM weight.

The 5 and 10% ANP-incorporated ANF membranes show ~72 and 64% area reduction after calcination, respectively, which is slightly less than the 75% area reduction observed in pure ANFs. As expected, incorporation of nanoparticles into alumina fibers reduces weight loss of membranes to ~65% for 5% ANP membranes and ~55% for 10% ANP membranes. This weight loss is much less than the 80% weight loss of the pure ANF membranes and can be attributed to the fact that ANPs do not lose weight during the heat treatment process, while the PVP component of the as-spun fibers evaporates and the AlAc part reacts with oxygen in air at high temperatures to form aluminum oxide.

SEM images in Figure 6 show the ANF morphologies before and after calcination. These images reveal that as-spun fibers

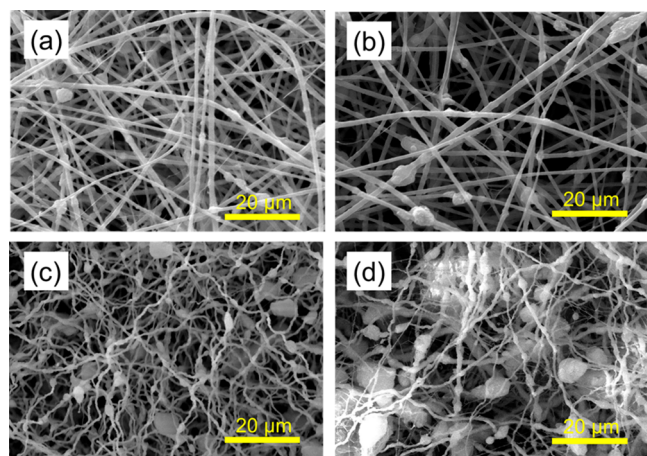


Figure 6. SEM microphotographs of PVP/AlAc fibers incorporated with ANPs: (a) 5%, as-spun; (b) 10%, as-spun; (c) 5%, calcined; (d) 10%, calcined.

have a uniform diameter and the nanoparticles are well-distributed inside the fibers, with some aggregations protruded from the fibers. After calcination, the diameter of fibers decreases and more nanoparticles become exposed to the surface that makes the aggregations more evident. Besides, the as-spun fibers in panels a and b of Figure 6 obtain a wavy structure after calcination shown in panels c and d of Figure 6. This change of morphology can be attributed to the effect of ANPs present in the fibers because, as shown in panels b and c

of Figure 5, the same linear fiber structure was shown before and after calcination of alumina fibers with no nanoparticle incorporated.

The ANP-incorporated ANFs were fabricated at weight ratios of 5:11.1 and 10:11.1 between ANPs and the alumina precursor, leading to more ANPs being embedded in the latter. The prepared 10% ANP-incorporated ANF membrane contains ~28.5 mg more ANPs compared to the 5% ANP-incorporated ANF membrane. That will have a noticeable effect on the properties of fibers because the membrane containing more ANPs possesses a higher solution uptake capacity, ~8% less area reduction, and ~10% less weight loss. The SEM images of alumina fibers impregnated with 5 and 10% ANP shown in panels c and d of Figure 6 confirm the presence of more nanoparticles and more aggregations along the fibers with a higher density of incorporated nanoparticles. The lower mechanical integrity of 10% ANP-incorporated alumina fibers compared to its 5% ANP counterpart can be attributed to the smaller diameter of ANFs in the case of 10% ANP, as seen in panels c and d of Figure 6. The 10% less weight loss of the fiber membrane with the higher ANP concentration is probably due to the higher ratio between ANPs, keeping their weight throughout the calcination process, and fiber material that loses weight during conversion from AlAc/PVP material to aluminum oxide.

Gas experiments were performed with 5 and 10% ANP-incorporated ANFs weighing 140 mg and loaded with 30 mg of PPM. The performance of these membranes is demonstrated in Figure 7, which shows superior performance in activating the

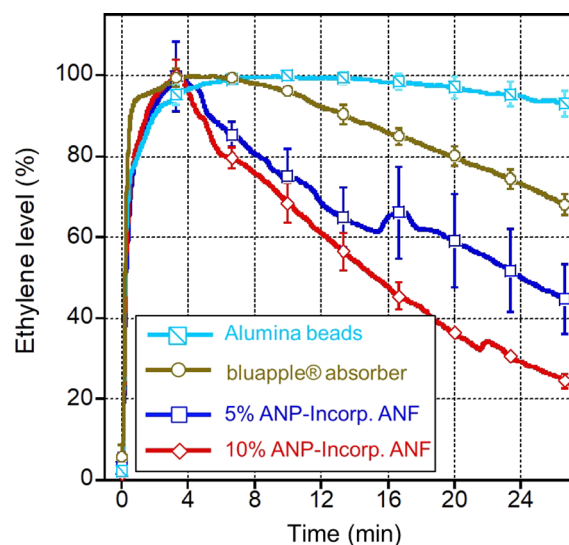
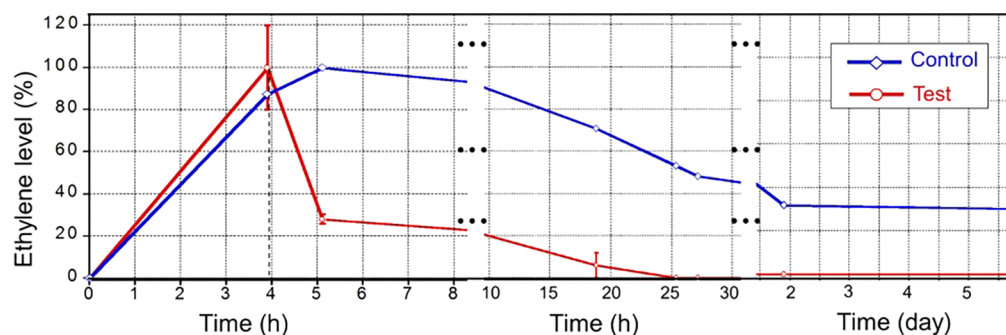


Figure 7. Ethylene absorption profiles of the 5 and 10% ANP-incorporated ANF membranes, alumina beads, and bluapple commercial absorber (vertical bars represent the SD of three tests).

salt absorber compared to the previous carriers (ANP only and ANP-incorporated CNF membrane) depicted in Figure 4. For 5 and 10% ANP-incorporated ANFs, the results in Figure 7 show an ethylene level reduction of 39 and 51% at 15 min increasing to 54 and 74% ethylene reduction at 25 min, respectively. It is worth mentioning that the two “bumps” on the curves for ANP-incorporated ANF membranes appear when the opposite side of the bag comes in contact with the probe tip and causes blocking. The brief clogging of the ethylene analyzer probe usually causes a small peak that lasts for

Table 1. Ethylene Absorption Capacity for Various Absorbers: Ethylene Level Percent at Multiple Time Points (Values Represent the Average and SD for $n = 3$)

	ethylene level (%)				
	5 min	10 min	15 min	20 min	25 min
ANP-incorporated CNF	96.8 ± 7.4	91.4 ± 9.6	86.7 ± 8.6	83.3 ± 6.5	80.2 ± 3.5
5% ANP-incorporated ANF	91.9 ± 6.8	75.3 ± 6.9	61.8 ± 7.4	59 ± 11.5	47.9 ± 9.3
10% ANP-incorporated ANF	88.6 ± 4.7	68.5 ± 5.1	50.9 ± 3.9	36.3 ± 0.7	27.6 ± 1.3
alumina beads	98.0 ± 1.7	99.9 ± 0.6	98.8 ± 1.4	96.9 ± 2.7	93.8 ± 3.6
bluapple absorber	99.7 ± 1.4	96.2 ± 1.0	87.7 ± 2.4	80.1 ± 2.3	71.3 ± 2.6

**Figure 8.** Long-term absorption of ethylene gas emitted from avocado fruits through using 5% ANP-incorporated ANF membrane. Membranes were placed into the test bags at 3.9 h, indicated by vertical dashed lines.

a few minutes if it is not resolved properly. On the basis of these results, it is feasible to tune the ethylene absorption capacity and kinetics of our ANP-incorporated ANF membranes simply by controlling the weight ratio between ANPs and alumina fiber material. Further, a comparison of ethylene absorption between alumina (10% ANP-incorporated ANF) and CNF incorporating a roughly equal amount of ANPs (~100–110 mg) indicates that the carrier material also plays a role in ethylene absorption characteristics. The ANP-incorporated ANFs even outperform powder form of ANPs (ANP only), which can be attributed to the larger surface area of ANPs and highly porous network as a result of the larger spacing between particles provided by the membrane.

3.3. Comparison to Conventional Ethylene Absorbers.

We have also compared the performance of our 10% ANP-incorporated ANF membranes to a similar weight of commercially available bluapple absorber (190 mg) and 140 mg alumina beads ($1/8$ in. diameter) loaded with 30 mg of PPM. Each experiment with either bluapple or alumina beads was performed 3 times, and the average and range of results plotted in Figure 7 show a satisfactory reproducibility. The results in Figure 7 demonstrate higher absorption efficiency of PPM on ANP-incorporated alumina fiber membranes compared to the bluapple absorber and alumina beads. A summary of results in Table 1 shows that bluapple beads compared to alumina beads absorb 4 and 17.4% more ethylene at 10 and 20 min, respectively. On the other hand, the ANP-incorporated CNF membrane (shown in Figure 4) and bluapple absorber have a comparable performance. The membrane absorbs more ethylene at the first 15 min, but the bluapple starts to overtake after that as a result of its higher rate of absorption. Finally, both 5 and 10% ANP-incorporated ANF membranes possess a significantly higher absorption capacity than the other absorbers. For instance, ANP (5 and 10%)–ANF membranes have absorbed 46.3 and 65% of ethylene at 20 min, respectively. However, the bluapple absorber has absorbed only 21.7% at 20 min, which is between one-half and one-third of the ethylene

amount absorbed by ANP–ANF membranes. Moreover, our experiments substantiate the possibility of controlling the absorption capacity and the rate of absorption from these membranes that can be achieved by controlling the concentration of ANPs incorporated into the fibers. Another feature of absorption from ANP–ANF membranes is the relatively higher absorption of ethylene during the first 3 min after releasing the membranes. This property can be very useful in situations where targeted fruits or vegetables are in the stage of their ripening process that is associated with burst ethylene production.²⁰ In such cases, the higher initial ethylene absorption from ANP–ANF membranes would first absorb the high level of ethylene (can be tens of parts per million depending upon the fruit)⁵⁴ accumulated around the products and then control the continuous production of ethylene through its large capacity and high absorption rate.

3.4. Membrane Effect on Absorption of Ethylene Emitted from Avocados.

Several experiments were performed to evaluate the impact of our membrane in bags containing avocados (for quantitative studies) and in bags containing bananas (for qualitative studies). Results of the experiment with avocados (see the Experimental Section for more details) reported in Figure 8 indicate that ethylene was built up in the test bags at an average rate of $3.8 \mu\text{L/h}$ per single avocado (equivalent to $24.88 \mu\text{L/h}$ per kg), reaching 13.5 ppm (100%) before we introduce the membranes into the bags at 3.9 h, indicated by a vertical dashed line in the figure. A single piece of membrane (5% ANP-incorporated ANF) weighing ~230 mg loaded with 60 mg of PPM was placed in each test bags, while the control bag was just opened and closed to count in induced air displacement when inserting the membranes in the test bags. Analyzing the gas inside the test bags after membrane insertion reveals a sharp 87% drop of the ethylene level within 1.2 h, followed by a more gradual ethylene reduction until no ethylene is left in the test bags at 21.5 h after introducing membranes. The zero ethylene concentration in the test bags was maintained for the rest of the test period (5

days), as shown in Figure 8. However, for the control, the ethylene level was still increasing ~13% within the same 1.2 h period. After 5 h, the ethylene level was gradually decreased, which can indicate that the fruit has passed its climacteric peak, and its rate of ethylene production is therefore decreasing as it ripens.^{55–59} This control result suggests that the ethylene level can be reduced to ~53% of the ethylene peak level naturally without any external absorber within 20 h after the climacteric peak, but the absorber membranes does make a noticeable impact in lowering the ethylene level as the test bags have reached zero ethylene concentration in the same 20 h window. This experiment continued for 6 days in total, and on day 6 (5 days after introducing the membrane), the test bags still had an average ethylene of 0.0 ppm, while the ethylene level in the control bag was 31% (equivalent to 8.6 ppm). Lowering the ethylene level at the right time before it reaches the climacteric peak is of paramount importance because it can suppress the autoinductive rise of ethylene production, accelerating senescence in fruits and vegetables.^{56,60}

The qualitative impact of our 5% ANP-incorporated ANF membrane in bags was evaluated using banana as the target fruit (see the Experimental Section for more details). Results shown in Figure 9 reveal only very minor visual differences between

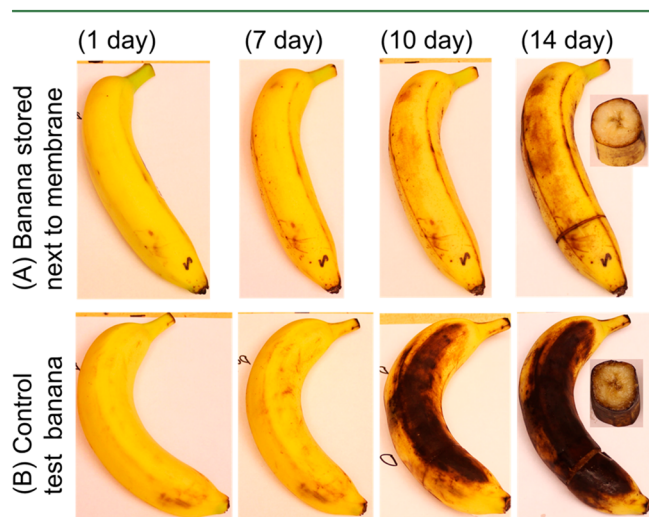


Figure 9. Photographs of a banana stored in a zip-lock bag (A) containing 5% ANP-incorporated ANF membrane and (B) with no absorber placed in the bag (control test), after 1, 7, 10, and 14 days.

the test and control bananas after 1 and 7 days. However, after 10 days, a dramatic difference is observed between the banana with the absorber (Figure 9A) appearing significantly fresher than the control banana (Figure 9B), which exhibits a large dark brown region on its skin. This diversion in the appearance of the two bananas that occurs starting on day 7 can be attributed to a sharp increase in the ethylene production and cellular respiration of bananas as a climacteric fruit. The quality difference is also apparent from the cross-section images of bananas on day 14 of the test, shown in Figure 9. In fact, the flesh of the banana placed next to the membrane is significantly firmer and has shallower bruising compared to the control test banana. This test demonstrates the effectiveness of our fiber membrane in prolonging the storage lifetime of products, potentially leading to cost savings associated with delivery, storage, and waste disposal of products.

As presented in this paper, developed membrane-based absorber systems have the capability to absorb relatively large amounts of ethylene in a short time and maintain a zero or low-ethylene concentration over an extended time period of at least 5 days, as demonstrated by our experimental results for 5% ANP-incorporated ANF. The large absorption capacity of membranes can be attributed to their higher surface area with a highly micro-/nanoporous network compared to conventional approaches, such as alumina beads. It is worth mentioning that the membranes have a PPM uptake capacity of ~21% of their weight, while ~3 mm beads showed a maximum uptake capacity of ~10% of their weight, and larger beads (5 mm diameter) have been reported to have a maximum uptake of only ~6%. Membranes also allow users to choose and customize an absorber based on the application (transportation, storage, etc.). ANP-incorporated CNFs are ~15% lighter than ANP-incorporated ANFs, making them a good choice in certain challenging applications, such as fruit container transportation, where a PPM–alumina bead package of larger than 1 kg would be needed to absorb high levels of ethylene.²⁴

Ultimately, the cost of manufacturing membranes at a large scale will be a key factor in commercial viability of each proposed membrane. Disregarding the costs of raw materials, making ANFs needs a one-time 2 h heat treatment in air at a maximum temperature of 700 °C that makes it more cost-effective than fabrication of CNFs requiring argon gas and a two-step heat treatment process that takes around 10 h and reaches 1000 °C. Incorporation of ANP will obviously add some additional costs that can be avoided if pure ANFs are to be used. Further optimization of the fabrication process along with a comparison of long-term performance and ease of fabrication between our membranes and commercial absorber products is the subject of our next research phase. Some of commercial products (sachets, films, or filters) are Dri-Fresh Fresh-Hold EA labels (Sirane, Ltd., U.K.), CJS (CJS Ethylene Filters), Purafil (Purafil, Inc., Doraville, GA, U.S.A.), Delta-Track (DeltaTrack, Inc.), and Ethylene Control (Ethylene Control, Inc.). Despite the different compositions of developed membranes, they share specific characteristics, such as a distinctly large surface area enhancing the absorption of ethylene by the substrate, planar form, flexibility, ease of handling, and lightweight, that distinguishes them from other absorber systems and makes them ideal for being used inside packaging materials. In conclusion, ANP-incorporated ANF/CNF membranes provide great potential for the commercial use as a packaging material by not only outperforming current commercial products but also providing a self-supporting vehicle unlike current beads-in-pouch commercial products.

■ ASSOCIATED CONTENT

📄 Supporting Information

The Supporting Information is available free of charge on the ACS Publications website at DOI: 10.1021/acs.jafc.7b05037.

Results of ethylene absorption experiments performed with CNF membranes and polymer membranes, each loaded with PPM (PDF)

■ AUTHOR INFORMATION

Corresponding Author

*E-mail: a.steckl@uc.edu.

ORCID

Daewoo Han: 0000-0002-0689-555X

Andrew J. Steckl: 0000-0002-1868-4442

Funding

This work was partially supported by the Cambridge Display Technology, Ltd. under Grant G401555-1012549. The authors also acknowledge support from the University of Cincinnati.

Notes

The authors declare no competing financial interest.

REFERENCES

- (1) Ben-Arie, R.; Sonego, L. Modified-atmosphere storage of kiwifruit (*Actinidia chinensis* Planch) with ethylene removal. *Sci. Hortic.* **1985**, *27*, 263–273.
- (2) McDonald, B.; Harman, J. Controlled-atmosphere storage of kiwifruit. I. Effect on fruit firmness and storage life. *Sci. Hortic.* **1982**, *17*, 113–123.
- (3) Agar, L.; Massantini, R.; Hess-Pierce, B.; Kader, A. Postharvest CO₂ and Ethylene Production and Quality Maintenance of Fresh-Cut Kiwifruit Slices. *J. Food Sci.* **1999**, *64*, 433–440.
- (4) Pesis, E.; Ackerman, M.; Ben-Arie, R.; Feygenberg, O.; Feng, X.; Apelbaum, A.; Goren, R.; Prusky, D. Ethylene involvement in chilling injury symptoms of avocado during cold storage. *Postharvest Biol. Technol.* **2002**, *24*, 171–181.
- (5) Awad, M.; Young, R. E. Postharvest variation in cellulase, polygalacturonase, and pectinmethylesterase in avocado (*Persea americana* Mill, cv. Fuerte) fruits in relation to respiration and ethylene production. *Plant Physiol.* **1979**, *64*, 306–308.
- (6) Dong, L.; Lurie, S.; Zhou, H.-W. Effect of 1-methylcyclopropene on ripening of 'Canino' apricots and 'Royal Zee' plums. *Postharvest Biol. Technol.* **2002**, *24*, 135–145.
- (7) Botondi, R.; DeSantis, D.; Bellincontro, A.; Vizovitis, K.; Mencarelli, F. Influence of ethylene inhibition by 1-methylcyclopropene on apricot quality, volatile production, and glycosidase activity of low-and high-aroma varieties of apricots. *J. Agric. Food Chem.* **2003**, *51*, 1189–1200.
- (8) Kader, A. A. Fruit maturity, ripening, and quality relationships. *Acta Hortic.* **1999**, *485*, 203–208.
- (9) Perkins-Veazie, P.; Clark, J.; Huber, D.; Baldwin, E. Ripening Physiology in 'Navaho' Thornless Blackberries: Color, Respiration, Ethylene Production, Softening, and Compositional Changes. *J. Am. Soc. Hortic. Sci.* **2000**, *125*, 357–363.
- (10) Scott, K.; McGlasson, W.; Roberts, E. Potassium permanganate as an ethylene absorbent in polyethylene bags to delay ripening of bananas during storage. *Aust. J. Exp. Agric.* **1970**, *10*, 237–240.
- (11) Kevany, B. M.; Tieman, D. M.; Taylor, M. G.; Cin, V. D.; Klee, H. J. Ethylene receptor degradation controls the timing of ripening in tomato fruit. *Plant J.* **2007**, *51*, 458–467.
- (12) Jeffery, D.; Smith, C.; Goodenough, P.; Prosser, I.; Grierson, D. Ethylene-independent and ethylene-dependent biochemical changes in ripening tomatoes. *Plant Physiol.* **1984**, *74*, 32–38.
- (13) Herner, R.; Sink, K. Ethylene production and respiratory behavior of the rin tomato mutant. *Plant Physiol.* **1973**, *52*, 38–42.
- (14) Roberts, J. A.; Schindler, C. B.; Tucker, G. A. Ethylene-promoted tomato flower abscission and the possible involvement of an inhibitor. *Planta* **1984**, *160*, 159–163.
- (15) Fuchs, Y.; Gorodeiski, N. The course of ripening of banana fruits stored in sealed polyethylene bags. *Am. Soc. Hortic. Sci. J.* **1971**, *96*, 401–403.
- (16) Ku, H. S.; Suge, H.; Rappaport, L.; Pratt, H. K. Stimulation of rice coleoptile growth by ethylene. *Planta* **1970**, *90*, 333–339.
- (17) Yang, S. F.; Hoffman, N. E. Ethylene biosynthesis and its regulation in higher plants. *Annu. Rev. Plant Physiol.* **1984**, *35*, 155–189.
- (18) Watkins, C. B. Ethylene synthesis, mode of action, consequences and control. In *Fruit Quality and Its Biological Basis*; Knee, M., Ed.; Academic Press: Sheffield, U.K., 2002; pp 180–224.
- (19) Abeles, F. B.; Morgan, P. W.; Saltveit, M. E., Jr. *Ethylene in Plant Biology*; Academic Press: San Diego, CA, 2012; DOI: DOI: 10.1016/C2009-0-03226-7.
- (20) Chervin, C.; El-Kereamy, A.; Roustan, J.-P.; Latché, A.; Lamon, J.; Bouzayen, M. Ethylene seems required for the berry development and ripening in grape, a non-climacteric fruit. *Plant Sci.* **2004**, *167*, 1301–1305.
- (21) Liu, Z.-X.; Park, J.-N.; Abdi, S. H.; Park, S.-K.; Park, Y.-K.; Lee, C. W. Nano-sized carbon hollow spheres for abatement of ethylene. *Top. Catal.* **2006**, *39*, 221–226.
- (22) Bailén, G.; Guillén, F.; Castillo, S.; Serrano, M.; Valero, D.; Martínez-Romero, D. Use of activated carbon inside modified atmosphere packages to maintain tomato fruit quality during cold storage. *J. Agric. Food Chem.* **2006**, *54*, 2229–2235.
- (23) Suslow, T. Performance of zeolite based products in ethylene removal. *Perishables Handl. Q.* **1997**, *92*, 32–33.
- (24) Wills, R.; Warton, M. Efficacy of potassium permanganate impregnated into alumina beads to reduce atmospheric ethylene. *J. Am. Soc. Hortic. Sci.* **2004**, *129*, 433–438.
- (25) Cazalet, M. F. Container for prevention of postharvest decay, maturation and senescence of harvested crops. U.S. Patent 4,235,750 A, Nov 25, 1980.
- (26) MacDonald, J. G.; McGrath, K. P.; Wu, B.; Kim, J.; Huang, L.; Greene, S. L.; Fish, J. E.; Hu, S.-H. Durable charged particle coatings and materials. U.S. Patent 7,141,518 B2, Nov 28, 2006.
- (27) MacDonald, J. Metal ion modified high surface area materials for odor removal and control. U.S. Patent 20120202684 A1, April 30, 2002.
- (28) Magargee, R.; Ahrens, W.; Eyde, D.; Smith, B. Sodium permanganate ethylene absorption agent. U.S. Patent 20060070523 A1, Oct 4, 2004.
- (29) Zagory, D. Ethylene-removing packaging. In *Active Food Packaging*; Rooney, M. L., Ed.; Springer: Boston, MA, 1995; pp 38–54, DOI: DOI: 10.1007/978-1-4615-2175-4_2.
- (30) Martínez-Romero, D.; Bailén, G.; Serrano, M.; Guillén, F.; Valverde, J. M.; Zapata, P.; Castillo, S.; Valero, D. Tools to maintain postharvest fruit and vegetable quality through the inhibition of ethylene action: A review. *Crit. Rev. Food Sci. Nutr.* **2007**, *47*, 543–560.
- (31) Ozdemir, M.; Floros, J. D. Active Food Packaging Technologies. *Crit. Rev. Food Sci. Nutr.* **2004**, *44*, 185–193.
- (32) Hu, L.; Martin, H. M.; Strathmann, T. J. Oxidation kinetics of antibiotics during water treatment with potassium permanganate. *Environ. Sci. Technol.* **2010**, *44*, 6416–6422.
- (33) Naik, P. N.; Chimatadar, S. A.; Nandibewoor, S. T. Kinetics and oxidation of fluoroquinolone antibacterial agent, norfloxacin, by alkaline permanganate: A mechanistic study. *Ind. Eng. Chem. Res.* **2009**, *48*, 2548–2555.
- (34) Willhite, C.; Bhat, V.; Ball, G.; McLellan, C. Emergency Do Not Consume/Do Not Use concentrations for potassium permanganate in drinking water. *Hum. Exp. Toxicol.* **2013**, *32*, 275–298.
- (35) Biji, K. B.; Ravishankar, C. N.; Mohan, C. O.; Srinivasa Gopal, T. K. Smart packaging systems for food applications: A review. *J. Food Sci. Technol.* **2015**, *52*, 6125–6135.
- (36) Prasad, P.; Kochhar, A. Active packaging in food industry: A review. *IOSR J. Environ. Sci., Toxicol. Food Technol.* **2014**, *8*, 01–07.
- (37) Dobrucka, R.; Cierpiszewski, R. Active and intelligent packaging food—Research and development—A review. *Pol. J. Food Nutr. Sci.* **2014**, *64*, 7–15.
- (38) East, A. R.; Samarakoon, H. C.; Pranamornkith, T.; Bronlund, J. E. A Review of Ethylene Permeability of Films. *Packag. Technol. Sci.* **2015**, *28*, 732–740.
- (39) Savoie, E.; Gagnon, J.; Doyon, G.; Brunet, F. Evaluation of the ethylene permeability of polyvinyl chloride (PVC). *Packag. Technol. Sci.* **1993**, *6*, 195–202.
- (40) Piergiorganni, L.; Scolaro, M.; Fava, P. Measurement of ethylene permeability of plastic films. *Packag. Technol. Sci.* **1992**, *5*, 189–196.
- (41) Wang, Y.; Eastal, A. J.; Chen, X. D. Ethylene and oxygen permeability through polyethylene packaging films. *Packag. Technol. Sci.* **1998**, *11*, 169–178.
- (42) Kim, J. S.; Reneker, D. H. Polybenzimidazole nanofiber produced by electrospinning. *Polym. Eng. Sci.* **1999**, *39*, 849–854.

- (43) Li, D.; Xia, Y. Electrospinning of nanofibers: Reinventing the wheel? *Adv. Mater.* **2004**, *16*, 1151–1170.
- (44) Agarwal, S.; Greiner, A.; Wendorff, J. H. Electrospinning of manmade and biopolymer nanofibers—Progress in techniques, materials, and applications. *Adv. Funct. Mater.* **2009**, *19*, 2863–2879.
- (45) Han, D.; Steckl, A. J. Superhydrophobic and oleophobic fibers by coaxial electrospinning. *Langmuir* **2009**, *25*, 9454–62.
- (46) Han, D.; Steckl, A. J. Triaxial electrospun nanofiber membranes for controlled dual release of functional molecules. *ACS Appl. Mater. Interfaces* **2013**, *5*, 8241–5.
- (47) Krewski, D.; Yokel, R. A.; Nieboer, E.; Borchelt, D.; Cohen, J.; Harry, J.; Kacew, S.; Lindsay, J.; Mahfouz, A. M.; Rondeau, V. Human health risk assessment for aluminium, aluminium oxide, and aluminium hydroxide. *J. Toxicol. Environ. Health, Part B* **2007**, *10*, 1–269.
- (48) World Health Organization (WHO). *The International Programme on Chemical Safety*; WHO: Geneva, Switzerland, 1995.
- (49) Cristescu, S. M.; Mandon, J.; Arslanov, D.; De Pessemier, J.; Hermans, C.; Harren, F. J. Current methods for detecting ethylene in plants. *Ann. Bot.* **2013**, *111*, 347–360.
- (50) Mitchell, R. R.; Gallant, B. M.; Thompson, C. V.; Shao-Horn, Y. All-carbon-nanofiber electrodes for high-energy rechargeable Li–O₂ batteries. *Energy Environ. Sci.* **2011**, *4*, 2952–2958.
- (51) Chen, L. F.; Zhang, X. D.; Liang, H. W.; Kong, M. G.; Guan, Q. F.; Chen, P.; Wu, Z. Y.; Yu, S. H. Synthesis of nitrogen-doped porous carbon nanofibers as an efficient electrode material for supercapacitors. *ACS Nano* **2012**, *6*, 7092–7102.
- (52) Zhao, D.; Wang, T.; Han, D.; Rusinek, C.; Steckl, A. J.; Heineman, W. R. Electrospun carbon nanofiber modified electrodes for stripping voltammetry. *Anal. Chem.* **2015**, *87*, 9315–21.
- (53) Kim, C.; Yang, K. S. Electrochemical properties of carbon nanofiber web as an electrode for supercapacitor prepared by electrospinning. *Appl. Phys. Lett.* **2003**, *83*, 1216–1218.
- (54) Curry, E. A., *Ethylene in Fruit Physiology*, In 14th Annual Postharvest Conference, Yakima, Washington, 1998.
- (55) Paul, V.; Pandey, R.; Srivastava, G. C. The fading distinctions between classical patterns of ripening in climacteric and non-climacteric fruit and the ubiquity of ethylene—an overview. *J. Food Sci. Technol.* **2012**, *49*, 1–21.
- (56) Wills, R.; Golding, J. *Postharvest: an introduction to the physiology and handling of fruit and vegetables*. UNSW press, 2016
- (57) Gwanpua, S. G.; Qian, Z.; East, A. R. Modelling ethylene regulated changes in 'Hass' avocado quality. *Postharvest Biol. Technol.* **2018**, *136*, 12–22.
- (58) Skic, A.; Szymańska-Chargot, M.; Kruk, B.; Chylińska, M.; Pieczywek, P. M.; Kurenda, A.; Zdunek, A.; Rutkowski, K. P. Determination of the optimum harvest window for apples using the non-destructive biospeckle method. *Sensors* **2016**, *16*, 661.
- (59) Lima, J.; Sthel, M.; Marín, E.; Gatts, C.; Cardoso, S.; Campostrini, E.; Pereira, M.; Campos, A.; Massunaga, M.; Vargas, H. In *Ethylene and CO₂ emission rates in tropical fruits investigated by infrared absorption techniques*, Analytical Sciences/Supplements, Proceedings of 11th International Conference of Photoacoustic and Photothermal Phenomena, 2002; Japan Soc. Anal. Chem.: 2002; pp s534–s537.
- (60) Alexander, L.; Grierson, D. Ethylene biosynthesis and action in tomato: a model for climacteric fruit ripening. *J. Exp. Bot.* **2002**, *53*, 2039–2055.